



Preparation, structure, drug release and bioinspired mineralization of chitosan-based nanocomplexes for bone tissue engineering

Rong Zeng^{a,b}, Mei Tu^{a,b,*}, Hongwei Liu^a, Jianhao Zhao^{a,b}, Zhengang Zha^{b,c}, Changren Zhou^{a,b}

^aDepartment of Materials Science and Engineering, College of Science and Engineering, Jinan University, Guangzhou 510632, PR China

^bEngineering Research Center of Artificial Organs and Materials, Ministry of Education, Guangzhou 510632, PR China

^cGuangzhou Overseas Chinese Hospital, The First Affiliated Hospital of Jinan University, Guangzhou 510630, PR China

ARTICLE INFO

Article history:

Received 27 November 2008

Received in revised form 26 April 2009

Accepted 27 April 2009

Available online 10 May 2009

Keywords:

Chitosan

Nanocomplexes

Drug release

Bioinspired mineralization

Bone tissue engineering

ABSTRACT

Chitosan-based nanocomplexes with various forms were prepared by ionically crosslinking with tripolyphosphate (TPP) in different acidic media under mild conditions. It was found that the self-assembly and ionic interactions of chitosan and TPP were greatly affected by reaction media, and chitosan-based nanofibers could be obtained in adipic acid medium while nanoparticles were formed in acetic acid medium. Using bovine serum albumin (BSA) as a macromolecular model-drug, in vitro drug release studies indicated that chitosan-based nanofibers and nanoparticles exhibited a similar prolonged release profile. In addition, the bioinspired mineralization of both chitosan-based nanofibers and nanoparticles was carried out by soaking them in synthetic body fluids (SBF). Transmission electron microscopy (TEM) and X-ray Diffraction (XRD) results indicated that chitosan-based nanofibers have better inductivity for nano-hydroxyapatite formation than chitosan-based nanoparticles. The results suggested that biomimetic chitosan-based nanofibers with controlled release capacity of bioactive factors may be of use in bone tissue engineering for enhancing the bioactivity and bone inductivity.

© 2009 Elsevier Ltd. All rights reserved.

1. Introduction

Chitosan, a natural polysaccharide composed of β -(1 \rightarrow 4)-linked 2-amino-2-deoxy-D-glucopyranose (glucosamine) and 2-acetamido-2-deoxy-D-glucopyranose (acetylglucosamine), has attracted considerable attention in pharmaceutical and biomedical applications owing to its favorable biological properties such as low toxicity, biocompatibility, and biodegradability (Ravi Kumar, Muzzarelli, Muzzarelli, Sashiwa, & Domb, 2004). A number of methods have been developed to fabricate chitosan-based micro or nanoscale particles, fibers, hydrogels, membranes, and three-dimensional scaffolds, which can be used in various applications such as biosensors, drug delivery systems, non-viral vectors for gene transfection, tissue reconstruction and wound healing (Bhattarai, Edmondson, Veis, Matsen, & Zhang, 2005; Liu & Yao, 2002; Rao, Naidu, Subha, Sairam, & Aminabhavi, 2006; Yi et al., 2005). Since chitosan becomes positively charged in aqueous acidic solutions due to the protonation of the free amine groups below its pK_a ($pH < 6.2$), it can form a variety of complexes with natural or synthetic polyanions of various characteristics by the oppositely-charged electrostatic interactions. Numerous studies (Agnihotri,

Mallikarjuna, & Aminabhavi, 2004; Berger et al., 2004; Il'ina & Varlamov, 2005) have been carried out to investigate chitosan complexes because such complexes usually have some specific physical, chemical and biological properties, and the formation process of complexes is very simple and mild, avoiding the possible toxicity of chemical reagents and other undesirable effects.

It's well known that the formation of chitosan complexes in aqueous solutions depends not only on the degree of deacetylation and molecular weight of chitosan, the chemical structure of polyanions, but also on their reaction conditions, such as pH, acidic medium, ionic strength, concentration, mixed ratio, and duration and temperature of the interaction. By controlling the above factors, chitosan complexes with various structure and properties could be prepared for controlled-release oral drug delivery or localized delivery of specific bioactive factors in tissue engineering (Janes, Calvo, & Alonso, 2001; Shu & Zhu, 2002). Bodmeier, Chen, and Paeratakul (1989) reported the technique of preparing micro- or nano-particulate drug delivery systems using chitosan/TPP complexes. Chen, Wang, and Hon (2006) studied the influence of carboxylic acid solvents and the pH of chitosan solution on the structure and morphology of chitosan/poly(acrylic acid) complexes, and successfully prepared chitosan/poly(acrylic acid) complex nanofibers using a modified dropping method in adipic acid solution.

Recently, bioinspired design and manufacture of scaffolds for tissue engineering have received increasing interests to provide

* Corresponding author. Address: Department of Materials Science and Engineering, College of Science and Engineering, Jinan University, Guangzhou 510632, PR China. Tel./fax: +86 2085223271.

E-mail address: tumei@jnu.edu.cn (M. Tu).

the microenvironment similar to the natural extracellular matrix (ECM) for regenerative cells and tissues (Chung & Park, 2007; Ingber et al., 2006; Ma, 2008). The biomimetic scaffolds should not only possess a three-dimensional and well defined microstructure similar to ECM, but also provide the controlled delivery of specific bioactive factors to enhance and guide the regeneration process. Polymeric nanofibers mimicking the nano-fibrillar structure of native ECM collagen have been thought to enhance cell adhesion, migration, proliferation and differentiated function (Barnes, Sell, Boland, Simpson, & Bowlin, 2007; Toh et al., 2006). Thus, chitosan-based nanofibers with controlled release capacity may be helpful to form a biomimetic microenvironment similar to native ECM in tissue engineering. In this paper, chitosan-based nanocomplexes with various forms: nanofibers or nanoparticles were prepared by ionically crosslinking with TPP in different acidic media under mild conditions. Their structure and interactions were characterized by TEM, XRD and Fourier-transform infrared (FT-IR) spectroscopy. Chitosan-based nanocomplexes obtained were subjected to *in vitro* hydrolysis studies in order to investigate their behaviors of releasing bioactive molecules in physiological environment using BSA as a macromolecular model-drug. Since hydroxyapatite (HA, $\text{Ca}_{10}(\text{PO}_4)_6(\text{OH})_2$) as one of the major inorganic constituents of bones has been proven to be bioactive and osteoconductive, and be able to promote the attachment and growth of human osteoblast-like cells (Cengiz, Gokce, Yildiz, Aktas, & Calimli, 2008; Fathia, Hanifia, & Mortazavi, 2008), the formation of HA induced by chitosan-based nanocomplexes was investigated and compared by bioinspired mineralization in SBF, in order to examine their biological efficacy for bone tissue engineering.

2. Materials and methods

2.1. Materials

Chitosan (medium molecular weight, Brookfield viscosity: 200cps) was purchased from Aldrich, and refined twice by dissolving in dilute acetic acid solution then precipitating from dilute ammonia. Adipic acid was supplied by Sinopharm Chemical Reagent Co. Ltd. TPP was purchased from Guangzhou Chemical Reagent Factory. BSA was obtained from Sigma. All other reagents were of analytical grade and used as received.

2.2. Methods

2.2.1. Preparation of chitosan-based nanocomplexes

Chitosan was dissolved in 2% v/v acetic acid solution and 2% w/v adipic acid solution at a concentration of 0.1% w/v, respectively. TPP was also dissolved in double-distilled water at 0.1% w/v. The chitosan solution was then dropped into TPP solution at a volume ratio of 3:1 through a syringe needle (0.45 mm in diameter), and stirring for 1 h at room temperature. The ionically crosslinked chitosan-based nanocomplexes were obtained using the following procedure: the opalescent mixed solutions were ultra centrifuged, pre-frozen at liquid N_2 (-196°C) and then lyophilized. To remove the remaining acid, the lyophilized products were washed with 0.1 mol/L NaOH solution and double-distilled water, and then lyophilized again to obtain the final products.

2.2.2. Drug loading and *in vitro* release

Macromolecular model-drug (BSA) was dissolved into the chitosan solution before the incorporation of TPP solution at 1.8 mg/mL, and then followed the above procedure to prepare the BSA-loaded chitosan-based nanocomplexes. The amount of BSA entrapped in the nanocomplexes was calculated based on the difference between the total amount of BSA used and the amount of non-en-

trapped BSA remaining dissolved in the aqueous suspension. BSA-loaded nanocomplexes were separated from the aqueous suspending medium by ultra centrifugation at 20,000 rpm for 30 min. The amount of free BSA in the clear supernatant was measured by ultraviolet–visible (UV–VIS) spectroscopy at 280 nm using a Jasco V-550 spectrophotometer (Japan). The BSA loading efficiency was calculated from indicated below equation: BSA loading efficiency = (Total amount of BSA – free BSA in supernatant)/Total amount of BSA $\times 100\%$. Each experiment was performed in triplicate.

In order to investigate the behaviors of releasing bioactive molecules in physiological environment of the obtained chitosan-based nanocomplexes, about 50 mg BSA-loaded nanocomplexes were suspended in 50 ml Phosphate Buffered Saline (PBS) solution (pH 7.4) incubated on a shaking water-bath at $37.0 \pm 0.5^\circ\text{C}$, 50 rpm, and sampled at predetermined intervals with adding an equal volume of buffer solution to maintain a constant volume of releasing medium. After ultra centrifugation at 20,000 rpm for 30 min, the amount of released BSA in the supernatant was determined by UV–VIS spectrophotometric measurements at 280 nm (Polk, Amsden, Yao, Peng, & Goosen, 1994; Xu & Du, 2003). Each experiment was repeated in triplicate.

2.2.3. Formation of HA

The obtained chitosan-based nanocomplexes were soaked in SBF with ion concentrations (Na^+ 142.0, K^+ 5.0, Mg^{2+} 1.5, Ca^{2+} 2.5, Cl^- 147.8, HCO_3^- 4.2, HPO_4^{2-} 1.0, SO_4^{2-} 0.5 mmol/L) nearly identical to those of human blood plasma in sterile polyethylene containers at $37.0 \pm 0.5^\circ\text{C}$ for 7 days. The SBF was prepared by dissolving appropriate quantities of chemical reagents including NaCl, NaHCO₃, KCl, $\text{KH}_2\text{PO}_4 \cdot 3\text{H}_2\text{O}$, $\text{MgCl}_2 \cdot 6\text{H}_2\text{O}$, CaCl_2 and Na_2SO_4 in distilled water, buffered at pH 7.40 with tris(hydroxymethyl)aminomethane and hydrochloric acid, according to the procedure reported by Kokubo, Miyaji, Kim, and Nakamura (1996). After soaking, the samples were removed from the SBF, washed with distilled water and vacuum dried.

2.2.4. Characterization

The morphologies of chitosan-based nanocomplexes and bioinspired-mineralized chitosan-based nanocomplexes were observed by TEM (Philips, Tecnai-10, Netherlands). Their crystal structure was determined by XRD in a Rigaku D/max-3A diffractometer (Japan) using a $\text{Cu K}\alpha$ X-ray line at a scan rate of $8^\circ \cdot \text{min}^{-1}$. The chemical interaction between chitosan and TPP in nanocomplexes was measured by FT-IR spectroscopy (Bruker, Equinox-55, Germany) in KBr.

3. Results and discussion

3.1. Morphology and structure of chitosan-based nanocomplexes

TEM images of chitosan-TPP nanocomplexes formed by ionic crosslinking in different acidic media are shown in Fig. 1. It could be seen that chitosan-based nanofibers with the average diameter about 200 nm and the length up to several microns were formed in adipic acid medium, while nanoparticles with the average diameter about 150 nm were formed in acetic acid medium. The reaction acidic medium strongly affects the formation of nanocomplexes since the chemical steric structure and the hydrocarbon chain length of carboxylic acid used would greatly influence the configuration of chitosan and its interaction with TPP in aqueous solutions (Shamov, Bratskaya, & Avramenko, 2002), though adipic acid and acetic acid have similar pK_a values, 4.43 and 4.76, respectively. Adipic acid with the large chain length and two carboxylic groups could affect the dispersion of chitosan in aqueous solutions and

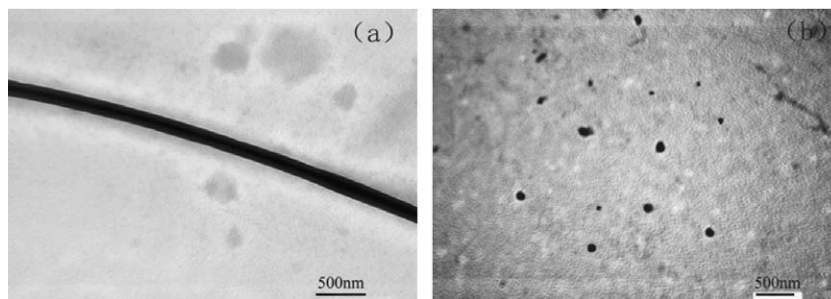


Fig. 1. TEM images of Chitosan-TPP nanocomplexes formed by ionically crosslinking in (a) adipic acid medium and (b) acetic acid medium.

the electrostatic interaction with TPP, and act as a template to induce the formation of nanofibers.

Fig. 2 demonstrates the XRD patterns of refined chitosan and chitosan-TPP nanocomplexes. The XRD pattern of chitosan-TPP nanoparticles obtained in acetic acid medium was similar to the pattern of frozen-dried refined chitosan in terms of the peak position and relative intensity, however the XRD pattern of chitosan-TPP nanofibers obtained in adipic acid medium showed a broad triplicate peak at 2θ of around 21° instead of a broad peak at 20.0° with a shoulder at 21.8° assigned to (0 2 0) and (1 0 2) reflection for chitosan-TPP nanoparticles, respectively. The new peak could be ascribed to the (0 1 1) reflection from adipic acid (Karadedeli, Bozkurt, & Baykal, 2005). The results indicated that there was some residue of adipic acid in chitosan-TPP nanofibers, which would influence the crystal structure of nanofibers.

Fig. 3 depicts the FTIR spectra of chitosan, chitosan-TPP nanofibers obtained in adipic acid media, chitosan-TPP nanoparticles obtained in acetic acid media, and TPP. From the pure chitosan spectrum, the carbonyl stretching (amide I band) at 1655 cm^{-1} and NH_2 bending (amide II band) at 1597 cm^{-1} could be clearly observed. The broad band ascribed to the stretching vibration of $-\text{NH}_2$ and $-\text{OH}$ group appeared at $3400\text{--}3500\text{ cm}^{-1}$, and the absorption bands at $1000\text{--}1200\text{ cm}^{-1}$ were attributed to its saccharine structure (Arof & Osman, 2003). Compared with that of chitosan, the absorption band assigned to the stretching vibration of $-\text{CH}_2-$ at 2920 cm^{-1} increased for chitosan-TPP nanocomplexes, and the amide II band shifted to 1574 cm^{-1} for chitosan-TPP nanoparticles, and further shifted to 1568 cm^{-1} for chitosan-TPP nanofibers, though the amide I band had almost no shift. The results indicated that some interaction have occurred between NH_2 groups of chitosan and TPP in the nanocomplexes. Moreover, the obvious difference of the relative intensity and position of amide II band to amide I band between nanoparticles and nanofibers also suggested that the interaction in chitosan-TPP nanoparticles was different from that in chitosan-TPP nanofibers.

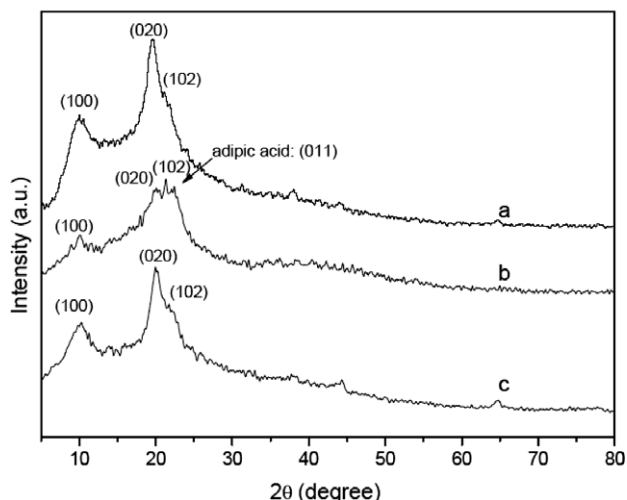


Fig. 2. XRD patterns of (a) chitosan, (b) chitosan-TPP nanofibers, and (c) chitosan-TPP nanoparticles.

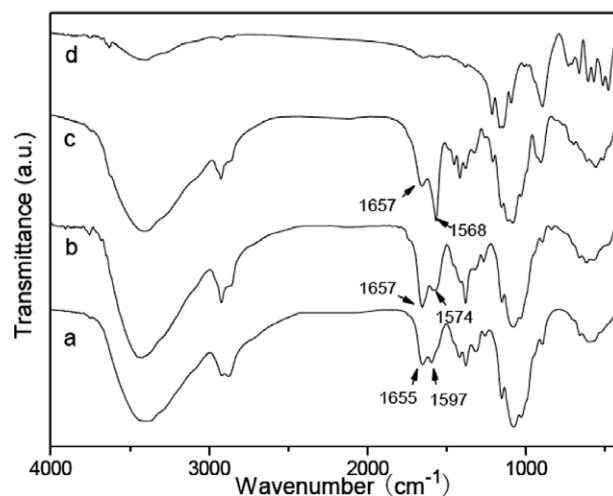


Fig. 3. FTIR spectra of (a) chitosan, (b) chitosan-TPP nanoparticles, (c) chitosan-TPP nanofibers, and (d) TPP.

fibers, though the amide I band had almost no shift. The results indicated that some interaction have occurred between NH_2 groups of chitosan and TPP in the nanocomplexes. Moreover, the obvious difference of the relative intensity and position of amide II band to amide I band between nanoparticles and nanofibers also suggested that the interaction in chitosan-TPP nanoparticles was different from that in chitosan-TPP nanofibers.

3.2. Model-drug in vitro release of chitosan-based nanocomplexes

Chitosan complex nano- or micro-particles formed by ionically cross-linking have been proven to be efficient delivery systems to deliver drugs and other biologically active components, such as peptides, proteins and oligonucleotides. In this work, according to the UV–VIS data, chitosan-TPP nanoparticles and nanofibers exhibited similar BSA loading efficiency values, 59.2% and 56.3%, respectively, since they had a similar loading mechanism. The results of BSA release from the BSA-loaded chitosan-based nanocomplexes in PBS at $37.0 \pm 0.5^\circ\text{C}$ are reported in Fig. 4. As can be seen, both chitosan-TPP nanoparticles and nanofibers exhibited a similar BSA releasing profile under experimental conditions, and the profile could be classified into three stages due to the complicated mechanisms for biodegradable polymeric delivery systems: diffusion of the drug and degradation of the polymer (Silva, Ducheyne, & Reis, 2007). The initial stage from 0 to 12 h was a burst release, caused by diffusion of BSA located closer to the surface of chitosan-TPP nanocomplexes. The second period from 12 to about 150 h was a minimal release stage, mainly caused by gradual degradation of

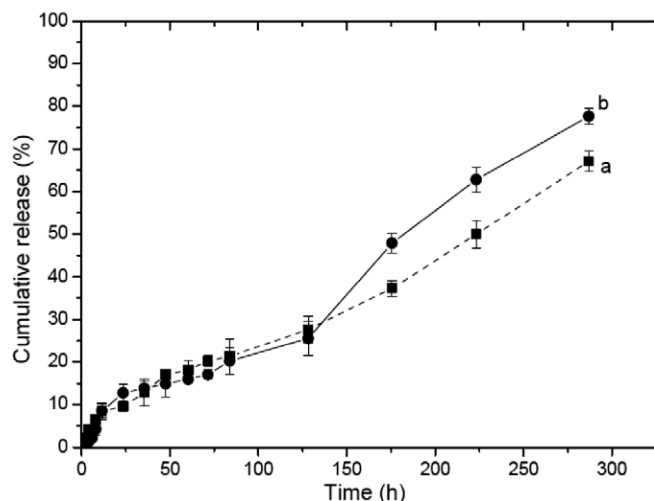


Fig. 4. Release of BSA from (a) chitosan-TPP nanoparticles and (b) chitosan-TPP nanofibers in PBS at 37.0 ± 0.5 °C.

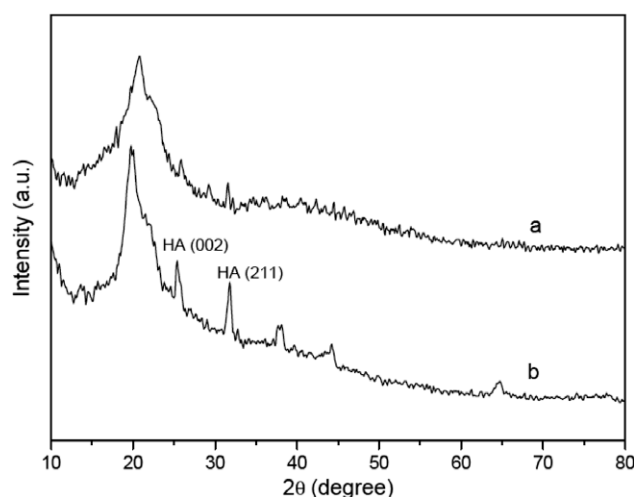


Fig. 5. XRD patterns of (a) chitosan-TPP nanoparticles and (b) chitosan-TPP nanofibers after soaking in SBF at 37.0 ± 0.5 °C for 7 days.

the chitosan-TPP nanocomplexes, and the third stage with the increased releasing rate of BSA was after about 150 h due to massive degradation of the material. Totally about 67.1% of BSA was released from the BSA-loaded chitosan-TPP nanoparticles within 280 h with a starting rate of 0.77%/h, while approximately 77.6% of BSA was released from the BSA-loaded chitosan-TPP nanofibers with a starting rate of 0.72%/h. The re-

sults suggested that chitosan-TPP nanofibers may provide a prolonged release of bioactive agents in physiological conditions as chitosan-TPP nanoparticles.

3.3. Bioinspired mineralization of chitosan-based nanocomplexes in SBF

Bioinspired mineralization of biomaterials by immersing in SBF has been frequently used to evaluate their in vitro bioactivity under physiological conditions for bone tissue engineering (Kokubo & Takadama, 2006). Fig. 5 shows the XRD patterns of bioinspired-mineralized chitosan-TPP nanocomplexes by soaking in SBF at 37.0 ± 0.5 °C for 7 days. Compared with chitosan-TPP nanoparticles, chitosan-TPP nanofibers after soaking in SBF showed new reflection peaks with higher relative intensity at 25.4° and 31.8° , which corresponded to the characteristic peaks of (0 0 2) and (2 1 1) planes of HA, respectively, indicating the presence of HA structure (Cengiz et al., 2008). The results indicated that chitosan-TPP nanofibers have better inductivity for hydroxyapatite formation than chitosan-based nanoparticles, which was confirmed by the TEM images of chitosan-TPP nanocomplexes after soaking in SBF for 7 days. As shown in Fig. 6, needle-like HA nanoparticles could be obviously observed only in chitosan-TPP nanofibers/SBF system. Since the natural bone is a composite mainly consisted of nano-sized, needle-like HA crystals (accounts for about 65 wt.% of bone) and collagen fibers (Olszta et al., 2007), chitosan-TPP nanofibers which not only mimic the nano-fibrillar structure of native ECM collagen but also have the ability to induce the formation of nano-HA in SBF may be used as a potential scaffolding material for bone tissue engineering.

4. Conclusion

Chitosan-based nanocomplexes with various forms were prepared by ionically crosslinking with TPP under mild conditions. It was found that the formation and structure of nanocomplexes were significantly affected by reaction media, and chitosan-TPP nanofibers mimicking the nano-fibrillar structure of native ECM collagen could be obtained in adipic acid medium while nanoparticles were formed in acetic acid medium. In vitro drug release of BSA in PBS indicated that both chitosan-TPP nanofibers and nanoparticles can provide a similar prolonged release of bioactive agents in physiological conditions. The results of bioinspired mineralization suggested that chitosan-TPP nanofibers have better inductivity for nano-hydroxyapatite formation than chitosan-TPP nanoparticles. It was supposed that biomimetic chitosan-TPP nanofibers with controlled release capacity of bioactive factors and inductivity for nano-HA formation may be used as a scaffolding material to provide a biomimetic microenvironment similar to the natural ECM for regenerative cells and tissues in bone tissue engineering.

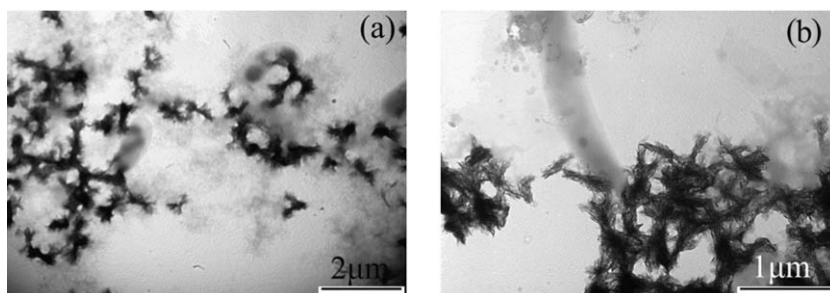


Fig. 6. TEM photos of (a) chitosan-TPP nanoparticles and (b) chitosan-TPP nanofibers after soaking in SBF at 37.0 ± 0.5 °C for 7 days.

Acknowledgements

The authors would like to acknowledge financial support from the National Natural Science Foundation of China (No. 20504018) and the National High Technology Research and Development Program of China (863 Program) (No. 2007AA09Z440).

References

- Agnihotri, S. A., Mallikarjuna, N. N., & Aminabhavi, T. M. (2004). Recent advances on chitosan-based micro- and nanoparticles in drug delivery. *Journal of Controlled Release*, 100, 5–28.
- Arof, A. K., & Osman, Z. (2003). FTIR studies of chitosan acetate based polymer electrolytes. *Electrochimica Acta*, 48, 993–999.
- Barnes, C. P., Sell, S. A., Boland, E. D., Simpson, D. G., & Bowlin, G. L. (2007). Nanofiber technology: Designing the next generation of tissue engineering scaffolds. *Advanced Drug Delivery Reviews*, 59, 1413–1433.
- Berger, J., Reist, M., Mayer, J. M., Felt, O., Peppas, N. A., & Gurny, R. (2004). Structure and interactions in covalently and ionically crosslinked chitosan hydrogels for biomedical applications. *European Journal of Pharmaceutics and Biopharmaceutics*, 57, 19–34.
- Bhattarai, N., Edmondson, D., Veis, O., Matsen, F. A., & Zhang, M. (2005). Electrospun chitosan-based nanofibers and their cellular compatibility. *Biomaterials*, 26, 6176–6184.
- Bodmeier, R., Chen, H., & Paeratakul, O. (1989). A novel approach to the oral delivery of micro- or nanoparticles. *Pharmacological Research*, 6, 413–417.
- Cengiz, B., Gokce, Y., Yildiz, N., Aktas, Z., & Calimli, A. (2008). Synthesis and characterization of hydroxyapatite nanoparticles. *Colloids and Surfaces A: Physicochemical and Engineering Aspects*, 322, 29–33.
- Chen, C.-Y., Wang, J.-W., & Hon, M.-H. (2006). Polyion complex nanofibrous structure formed by self-assembly of chitosan and poly(acrylic acid). *Macromolecular Materials and Engineering*, 291, 123–127.
- Chung, H. J., & Park, T. G. (2007). Surface engineered and drug releasing pre-fabricated scaffolds for tissue engineering. *Advanced Drug Delivery Reviews*, 59, 249–262.
- Fathia, M. H., Hanifia, A., & Mortazavi, V. (2008). Preparation and bioactivity evaluation of bone-like hydroxyapatite nanopowder. *Journal of Materials Processing Technology*, 202, 536–542.
- Il'ina, A. V., & Varlamov, V. P. (2005). Chitosan-based polyelectrolyte complexes: a review. *Applied Biochemistry and Microbiology*, 41, 5–11.
- Ingber, D. E., Mow, V. C., Butler, D., Niklason, L., Huard, J., Mao, J., et al. (2006). Tissue engineering and developmental biology: Going biomimetic. *Tissue Engineering*, 12, 3265–3283.
- Janes, K. A., Calvo, P., & Alonso, M. J. (2001). Polysaccharide colloidal particles as delivery systems for macromolecules. *Advanced Drug Delivery Reviews*, 47, 83–97.
- Karadedeli, B., Bozkurt, A., & Baykal, A. (2005). Proton conduction in adipic acid/benzimidazole hybrid electrolytes. *Physica B*, 364, 279–284.
- Kokubo, T., Miyaji, F., Kim, H. M., & Nakamura, T. (1996). Spontaneous formation of bonelike apatite layer on chemically treated titanium metals. *Journal of the American Ceramic Society*, 79, 1127–1129.
- Kokubo, T., & Takadama, H. (2006). How useful is SBF in predicting in vivo bone bioactivity? *Biomaterials*, 27, 2907–2915.
- Liu, W. G., & Yao, K. D. (2002). Chitosan and its derivatives—a promising non-viral vector for gene transfection. *Journal of Controlled Release*, 83, 1–11.
- Ma, P. X. (2008). Biomimetic materials for tissue engineering. *Advanced Drug Delivery Reviews*, 60, 184–198.
- Olszta, M. J., Cheng, X., Jee, S. S., Kumar, R., Kim, Y.-Y., Kaufman, M. J., et al. (2007). Bone structure and formation: A new perspective. *Materials Science and Engineering: R: Reports*, 58, 77–116.
- Polk, A., Amsden, B., Yao, K. D., Peng, T., & Goosen, M. F. A. (1994). Controlled release of albumin from chitosan-alginate microcapsules. *Journal of Pharmaceutical Sciences*, 83, 178–185.
- Rao, K. S. V. K., Naidu, B. V. K., Subha, M. C. S., Sairam, M., & Aminabhavi, T. M. (2006). Novel chitosan-based pH-sensitive interpenetrating network microgels for the controlled release of cefadroxil. *Carbohydrate Polymers*, 66, 333–344.
- Ravi Kumar, M. N. V., Muzzarelli, R. A. A., Muzzarelli, C., Sashiwa, H., & Domb, A. J. (2004). Chitosan chemistry and pharmaceutical perspectives. *Chemical Reviews*, 104, 6017–6084.
- Shamov, M. V., Bratskaya, S. Y., & Avramenko, V. A. (2002). Interaction of carboxylic acids with chitosan: effect of pK and hydrocarbon chain length. *Journal of Colloid and Interface Science*, 249, 316–321.
- Shu, X. Z., & Zhu, K. J. (2002). Controlled drug release properties of ionically cross-linked chitosan beads: The influence of anion structure. *International Journal of Pharmaceutics*, 233, 217–225.
- Silva, G. A., Ducheyne, P., & Reis, R. L. (2007). Materials in particulate form for tissue engineering. 1. basic concepts. *Journal of Tissue Engineering and Regenerative Medicine*, 1, 4–24.
- Toh, Y.-C., Ng, S., Khong, Y. M., Zhang, X., Zhu, Y., Lin, P.-C., et al. (2006). Cellular responses to a nanofibrous environment. *Nanotoday*, 1, 34–43.
- Xu, Y., & Du, Y. (2003). Effect of molecular structure of chitosan on protein delivery properties of chitosan nanoparticles. *International Journal of Pharmaceutics*, 250, 215–226.
- Yi, H., Wu, L.-Q., Bentley, W. E., Ghodssi, R., Rubloff, G. W., Culver, J. N., et al. (2005). Biofabrication with chitosan. *Biomacromolecules*, 6, 2881–2894.